Research Paper

Study of Magnetic Properties of Amorphous Fe-Mn-Zr Alloys

A PERUMAL*
Department of Physics, Indian Institute of Technology, Guwahati-781 039 (India)

(Received on 26 December 2005; Accepted on 07 March 2006)

We report the study of ac susceptibility, magnetization and magnetoresistivity in the temperature range of 4.2 K to 300 K and in the magnetic field up to 6 Tesla on amorphous $Fe_{90-x}Mn_xZr_{10}$ (x = 0~16) alloys. All the samples exhibit clear reentrant magnetic phase transition behaviour. The magnetic parameters such as coercivity, local magnetic anisotropy and high-field susceptibility are found to increase with Mn concentration. The magnetoresistivity study shows that remarkable effects due to magnetic ordering are present and the magnitude of spontaneous resistive anisotropy decreases with increasing Mn concentration. The present observations suggest that the antiferromagnetic coupling increases significantly with Mn concentration and described by an exchange frustration model. The obtained results provide conclusive evidence of weak-itinerant ferromagnetism for all the samples of present investigation.

Key words: Reentrant behaviour, Exchange frustration, Magnetic anisotropy, Magnetization, Spin glass, Magnetoresistivity, Spontaneous resistive anisotropy

Introduction

The study of magnetism in amorphous transition metal alloys with random mixture of competing exchange interactions has captured the attention of scientists[1]. The introduction of disorder, i.e., the random addition of antiferromagnetic (AFM) exchange interactions in the ferromagnetic (FM) Heisenberg system leads to a loss of FM order through the exchange frustration. At lower levels of exchange frustration, the system displays characteristics of both long-range FM order and spin-glass (SG) order. On warming such systems from low temperature, the SG order melts at a temperature T_{SG} followed by the loss of FM order at T_C.

Although such behaviour has been observed in number of systems, the amorphous alloys are found to be most suitable for the systematic study of these phenomena. Among various systems, amorphous (a-) $Fe_{90}Zr_{10}$ alloy exhibits a reentrant phenomenon (RSG), i.e., a transition from paramagnetic (PM) to FM state at a temperature, T_C, followed by another transition from FM to SG like state at lower temperature, T_{SG}. The reentrant transition from the FM state to the SG like state has been explained on the basis of spin canting in infinite range model with Heisenberg spins[2] and infinite 3D ferromagnetic network with finite spin clusters model[3]. Increasing Fe by 3 at% in a-$Fe_{90}Zr_{10}$ leads to a composition close to multi-critical point and doesn't allow one to study RSG behaviour in detail[4,5]. The replacement of Fe by other transition metal or metalloid elements in a-$Fe_{90}Zr_{10}$ alloy drastically changes the magnetic state[6] depending on nature of the substituting elements. The replacement of Mn exhibits RSG behaviour over a wide range of concentration and are suitable for the study of RSG[7]. The controversy surrounding the transition from PM to FM state in these alloys has been well debated[8]. However, the exact nature of the low temperature transition T_{SG} and that of RSG state has eluded clear-cut understanding so far.

Also, the low temperature galvanomagnetic properties of amorphous alloys and nanocrystals dispersed amorphous matrix have become a subject of renewed interest[9,10] due to the observation of giant magnetoresistance in some mixed exchange interaction systems. While the magnetoresistance (MR) of these alloys is predicted to be sensitive only to changes in magnetic correlation on a scale of order of electron mean free path, the magnetization depends on both short and long-range FM orders as well as on the rotation of FM domains as a response to applied magnetic field. Hence, the study of MR not only provides a unique way to obtain several important and fundamental parameters related to electron-transport properties, but also reveals complementary information about microscopic magnetization.

Thus, in the present investigation we report systematic temperature and field dependent magnetic and magnetoresistivity and ac susceptibility (ACS) measurements on a-$Fe_{90-x}Mn_xZr_{10}$ (x=0~16) alloys to understand (i) low temperature magnetic behaviour and (ii) relationship between magnetic interactions and electron-scattering mechanisms.

Experimental Details

Amorphous ribbons of $Fe_{90-x}Mn_xZr_{10}$ (0<x<16) about 1-2 mm wide and 20-30 μm thick were prepared by melt-spinning technique. The amorphous nature of the samples was confirmed through X-ray diffraction study. A

* E-mail: perumal@iitg.ernet.in

detailed composition analysis was determined through EDAX method and it was found to be close to the nominal composition of the alloy ingots. The thermoremanent and thermomagnetization measurements at different temperatures and fields were carried out on a single long ribbon sample using Quantum Design (MPMS model) SQUID magnetometer with a sensitivity of 10^{-11} A m^2 and vibration sample magnetometer (Oxford, Maglab model) with the sensitivity of 10^{-10} A m^2 for all samples over the temperature range 4.2 K to 300 K at various constant applied field values up to 5 MA/m. ACS measurement was carried out using the mutual induction method with field ranging from 80 to 4000 A/m and with frequency range from 80 Hz to 1 kHz. The set point temperature for each measurement was controlled with an accuracy of 20 mK by means of a proportional, integral, and derivative controller mechanism using Lake-Shore temperature controller. The resistivity measurements under zero-field and in-field were performed at a constant current of 10 mA in applied fields of up to 4 MA/m over the temperature range of 4.2 to 300 K employing the standard four probe dc technique. Considerable care was taken to ensure that the current-voltage contacts were collinear so that no Hall voltage component contributed to the magnetoresistive anisotropy. The magnetoresistance measurement was performed at various temperatures in both longitudinal and transverse geometries over the field range 0 to 4 MA/m.

Results and Discussion

Magnetization

Figure 1 shows the real (χ') and imaginary (χ'') components of ACS for a-$Fe_{90-x}Mn_xZr_{10}$ (x=0, 8, and 16) in an externally applied field of 1600 A/m with 80 Hz frequency. This figure clearly shows that all the samples studied in the present investigation exhibit well-defined RSG behaviour below room temperature. The broad nature of the ACS curve results in large uncertainty in determining both low and high temperature transitions. In order to obtain the correct values of T_{SG} and T_C, the ac field dependent [40 A/m (o), 400 A/m (x), and 1600 A/m (+)] measurements were performed close to the transition temperatures at constant (80 Hz) frequency, as shown in figure 2 for a-$Fe_{86}Mn_4Zr_{10}$ alloy. It could be clearly seen that the sharpness of the χ' peak observed close to transition temperatures are suppressed in higher applied ac fields. In addition, the lower transition temperature shifts to further lower temperature, while no significant shift has been observed in the high temperature transition with increasing ac field. The transition temperatures are obtained by extrapolating the field dependence of ACS data to zero-field. These data suggest that as Mn concentration increases, the FM region becomes narrower due to the decrease and increase in T_C (7 K/at.% Mn) and T_{SG} (3 K/at.% Mn), respectively. The

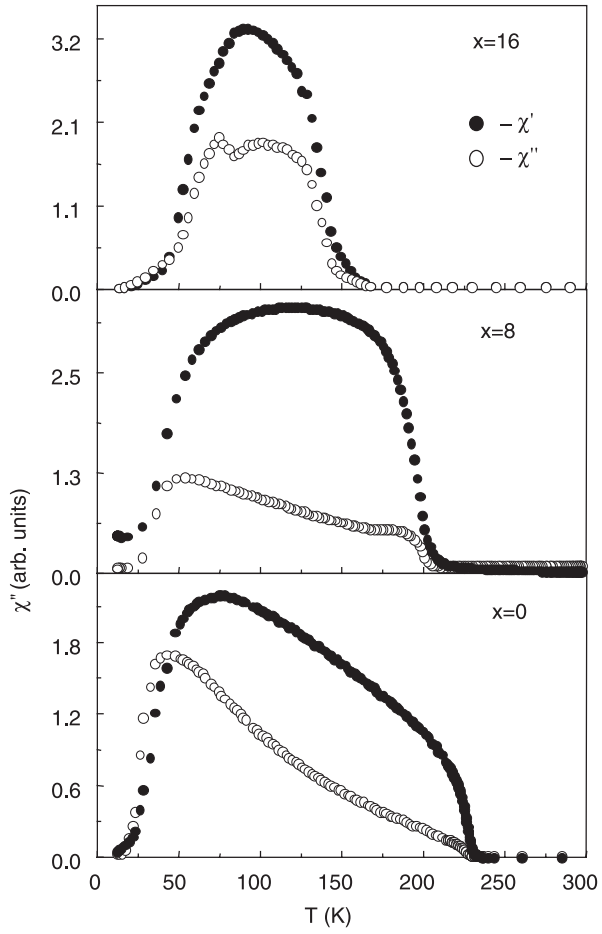

Figure 1: *The real (χ') and imaginary (χ'') components of ac susceptibility data measured in an applied field of 1600 A/m with 80 Hz frequency for a-$Fe_{90-x}Mn_xZr_{10}$ (x = 0, 8, 16) alloys*

frequency dependence of ACS data, as shown in figure 3, indicates the presence of spin-glass transition which seems to be a mixed state rather than a pure spin-glass state. These observations are in good agreement with the dc magnetization measurements[11] where the spontaneous magnetization does not go to zero at any temperature below T_C and the observation of freezing temperature provides conclusive evidence for the existence of a mixed-phase at low temperature. There are two ways in which a dopant can actively change the magnetization: (i) to change the Fe moment and (ii) to introduce the exchange interaction/frustration and drive the magnetic structure into collinear/non-collinear state. In order to understand the effect of Mn doping at low temperature, the field dependent magnetization curves were measured for all the samples at 4.2 K and depicted in figure 4. All the samples exhibit non-saturation behaviour at high-field region. The values of T_C and Fe magnetic moment (inset of Fig. 4) decrease with increasing Mn concentration. This suggests a possible presence of competing exchange interactions, which drives the system into non-collinear structure.

To understand the development of competing exchange interactions, the isothermal magnetization

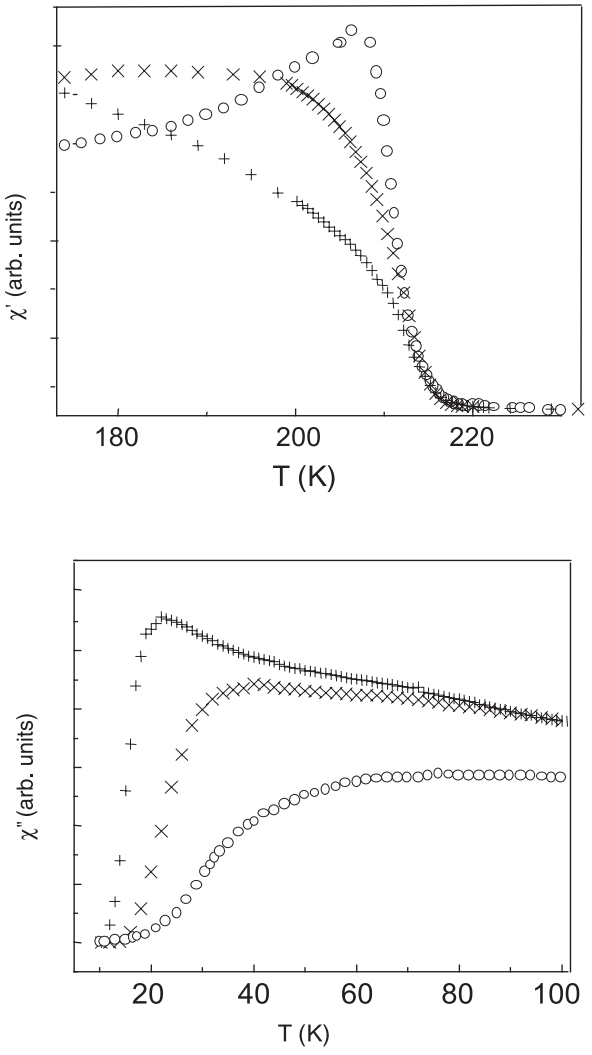

Figure 2: *The real (χ') and imaginary (χ'') components of ac susceptibility data measured in an applied field of 40 A/m (o), 400 A/m (×), and 1600 A/m (+) with 80 Hz frequency for a-$Fe_{86}Mn_4Zr_{10}$ alloy.*

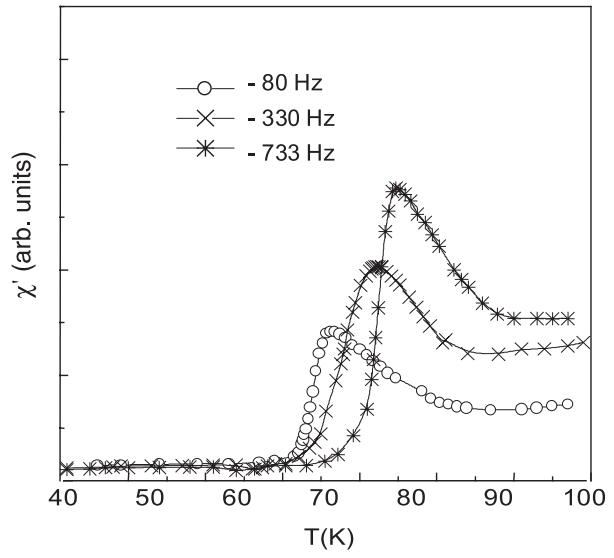

Figure 3: *The imaginary ((χ'') component of ac susceptibility data measured in an applied field of 1600 A/m with different frequencies 80 Hz (-o-), 330 Hz (-×-) and 733 Hz (-*-) for a-$Fe_{80}Mn_{10}Zr_{10}$ alloy*

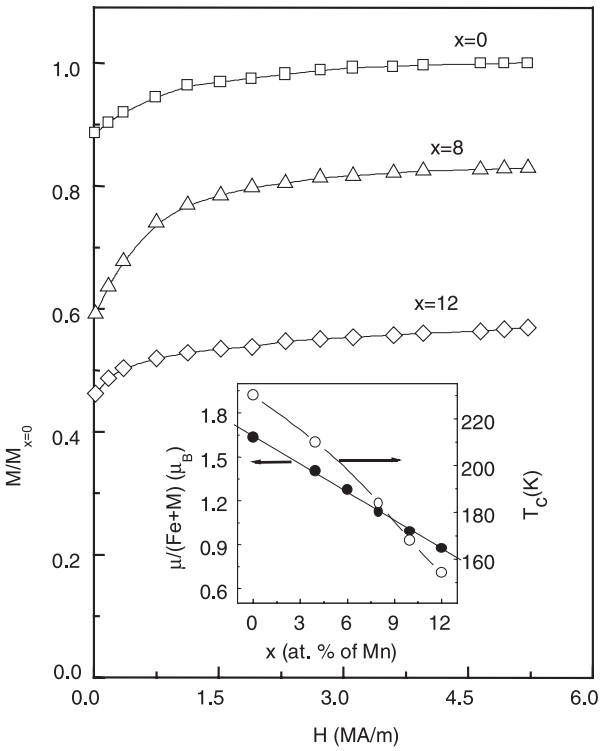

Figure 4: *The magnetic isotherms for a-$Fe_{90-x}Mn_xZr_{10}$ alloys. The magnetization axis is normalized with respect to the magnetization values at 5.2 MA/m for x=0. Inset: The composition dependent average magnetic moment and Curie temperature of a-$Fe_{90-x}Mn_xZr_{10}$ alloys*

curves at different temperatures for all the samples were measured and depicted in figure 5 for $Fe_{82}Mn_8Zr_{10}$ alloys together with temperature dependent coercivity data. The coercivity (Fig. 5b) starts to develop below T_C, however, a rapid increase is observed only just below T_{SG} where the ACS data shows the rapid decrement in its signal. In order to determine the high-field susceptibility (χ_{HF}) and local magnetic anisotropy (ζ), the magnetization curve is fitted by an analytical expression $M(H) = \chi_{HF}H+M(0)(1-\zeta H^{-\phi})$ which describes the approach of magnetization saturation[12]. Here M(0) defines the magnetization at zero-field and the local magnetic anisotropy is due to the pinning of AFM with FM spins. The calculated values of ζ is found to increase with Mn concentration, as shown in figure 6a and the χ_{HF}, so-called 'single domain susceptibility', exhibit a steep fall (Figure 6b) for temperatures just below T_C and attains a lower stable value at low temperatures. This is a typical character of the weak-itinerant ferromagnet[13,14]. The large value of χ_{HF} is another indication of itinerant character, which might be caused by the flipping of weakly coupled AFM spins under high magnetic field.

The coexistence of AFM and FM states could be identified through distance dependence Fe-Fe exchange interactions in Fe-Zr alloys[15]. It is well known that the spin moment on Fe atoms has a tendency to couple negatively when Fe atoms are densely packed.

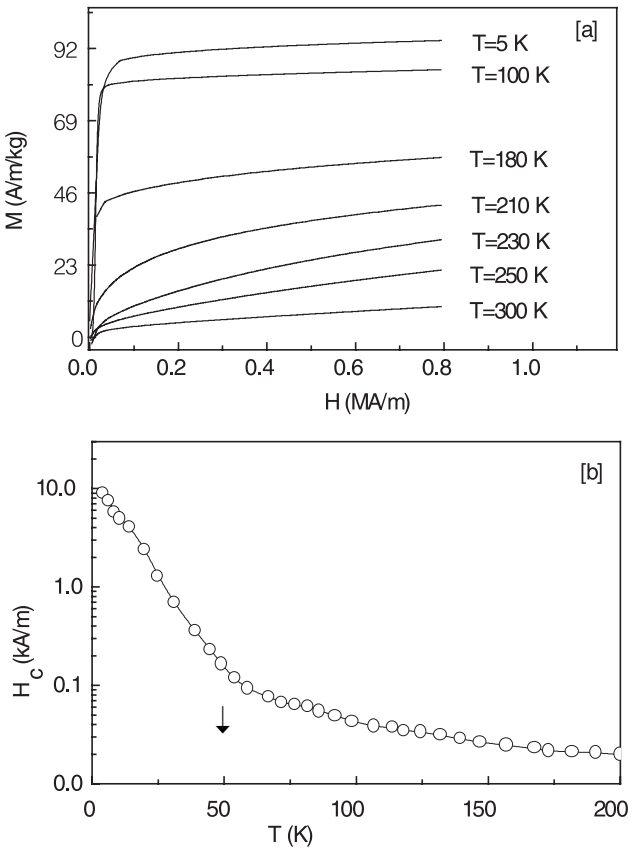

Figure 5: *(a) Magnetic isotherms at different temperatures and [b] temperature dependent coercivity for a-$Fe_{82}Mn_8Zr_{10}$ alloy.*

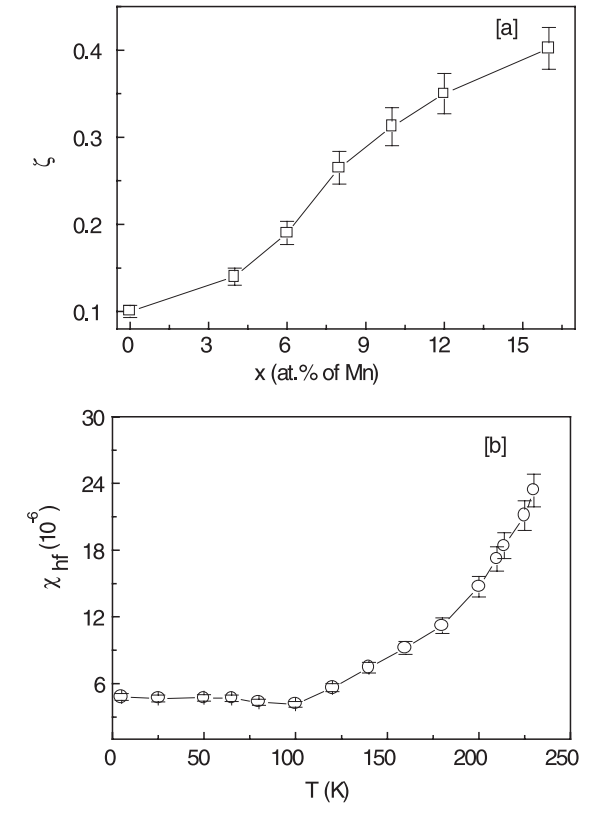

Figure 6: *(a) The local magnetic anisotropy constant as a function of Mn concentration for a-$Fe_{90-x}Mn_xZr_{10}$ alloys and (b) the high-field susceptibility as a function of temperature for a-$Fe_{82}Mn_8Zr_{10}$ alloy.*

Theoretical calculations also suggest that the amplitude and sign of local magnetic coupling depends strongly on the surrounding environments[16]. The Fe rich amorphous alloys seem to have a considerable amount of local atomic spin clusters based on nearly 12 fold coordinated dense random structure[17], which supports the presence of AFM exchange interactions. The replacement of Fe by small amount of Mn substitution would lead to the decrement in Fe-Fe pairs, but the substitution of Mn forms an AFM coupling between Fe and Mn (though AFM coupling between Fe-Mn is weaker than Fe-Fe), which has a tendency to reduce the magnetic moment and T_C as observed in the present investigation. The presence of AFM coupling regions is also evident from Mossbauer studies[18], where the development of a low-field peak has been observed in the hyperfine field distribution with increasing Mn concentration. This AFM coupling, arising from Fe-Fe and Fe-Mn exchange interactions, may lead to the non-collinear behaviour and might be responsible for the decrease in T_C and increase in ζ and χ_{HF}.

Magnetoresistivity

Since the MR provides a simple way to obtain (i) the relationship between magnetic interactions and electron-scattering mechanisms and (ii) the magnetic contribution to resistivity, the study of temperature and field dependence of MR have been discussed in the section below.

Figure 7 shows the longitudinal MR (LMR) and transverse MR (TMR) as a function of applied field for all the samples at selected temperatures: $T<T_{SG}$, $T_{SG}<T<T_C$, and $T>T_C$. The MR calculated in the present investigation is defined as

$$\left(\frac{\Delta\rho}{\rho}\right)_{(\perp)\ or\ (\parallel)} = \left[\frac{\rho(H,T)-\rho(0,T)}{\rho(0,T)}\right]_{(\perp)\ or\ (\parallel)} \quad \ldots (1)$$

where $\rho(H,T)$ is the resistance of the sample under the magnetic field at a particular temperature and ($\perp$) ($\parallel$) indicates the field applied in the transverse (longitudinal) direction. In all cases, it is seen that LMR is positive (solid circles in Fig. 7) and the magnitude of LMR decreases with increasing Mn concentration. This reduction could be attributed to the formation of zero-field regions in the sample due to an increase in AFM spins. In fact, the effect of competing interactions could be clearly observed in the form of a zero-field tail in a hyperfine field distribution[19]. The observed MR is smaller in the SG region than in the FM region and above T_C it becomes progressively smaller and takes on an approximate H^2 dependence. On the other hand, the TMR is negative (open circles in Fig. 7) at low field and crosses over to positive values at higher fields resulting in a minimum in TMR. The initial steep decrease (increase)

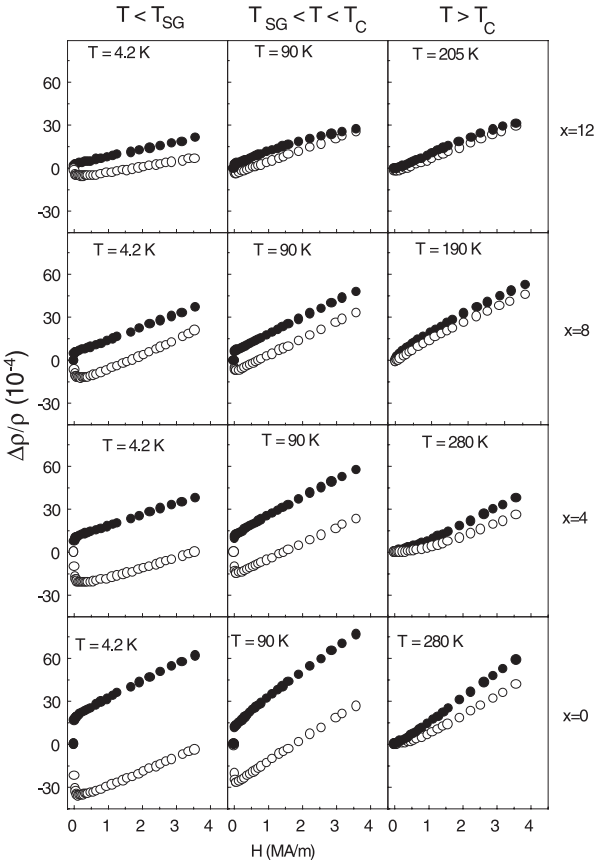

Figure 7: *Longitudinal (●) and transverse (o) magnetoresistance as a function of field for a-$Fe_{90-x}Mn_xZr_{10}$ alloys obtained at different temperatures: $T<T_{SG}$, $T_{SG}<T<T_C$, and $T>T_C$.*

of TMR (LMR) seems to be related to the FM character of the sample as it disappears above the Curie temperature.

The spontaneous resistive anisotropy (SRA) measures the difference in the resistivity of a ferromagnetic metal in zero induction when the magnetization is parallel or perpendicular to the current direction, as described by

$$\left(\frac{\Delta\rho}{\rho_0}\right)_{(s)} = \left[\left(\frac{\Delta\rho}{\rho_0}\right)_{\parallel(s)} - \left(\frac{\Delta\rho}{\rho_0}\right)_{\perp(s)}\right] \quad \ldots (2)$$

The determined values of SRA based on eqn.(2) is plotted as a function of temperature in figure 8. Here, we have not observed any nonzero SRA above T_C. This is anticipated since the system is far from its FM state and the applied field is not adequate to induce any appreciable changes in the polarization of spins at this temperature. On the other hand, a nonzero SRA is observed below T_C. The obtained SRA decreases not only with increasing Mn concentration, but also with increasing temperature for a particular concentration. According to the *two-current-conduction* model for weak-itinerant ferromagnetic system, the spin-up and spin-down electrons conduct in parallel and the SRA is a consequence of the anisotropic $d\uparrow$–$d\downarrow$ mixing caused

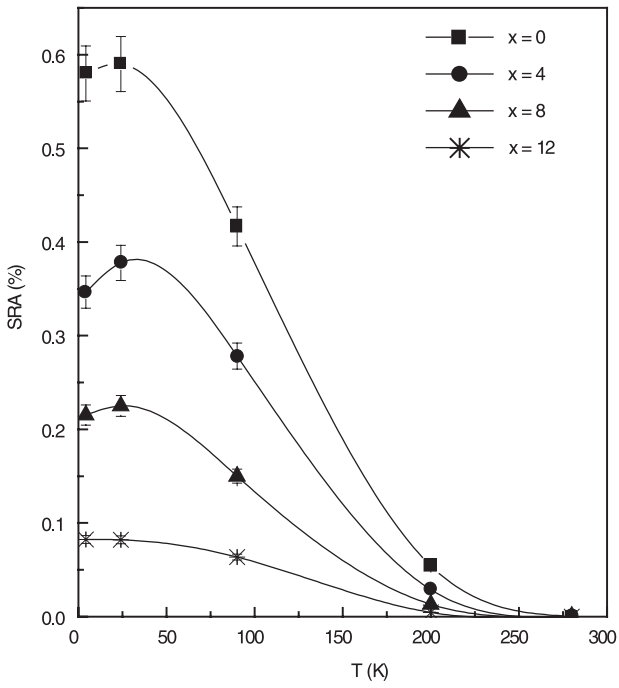

Figure 8: *Spontaneous resistive anisotropy as a function of temperature for a-$Fe_{90-x}Mn_xZr_{10}$ alloys*

by the spin-orbit interaction[20]. Calculations based on this model yield the following expressions for the SRA,

$$\left(\frac{\Delta\rho}{\rho_0}\right)_{(s)} = \gamma'\left(\frac{\rho^0_\downarrow - \rho^0_\uparrow}{\rho^0_\uparrow}\right) \quad \ldots (3)$$

Where, $\rho^0_\uparrow$ and $\rho^0_\downarrow$ are the residual resistivity for spin-up and spin-down electrons respectively. The value of γ' is estimated to be 0.01 for Fe and Ni based alloys. The eqn. (3) provides a criterion for determining whether a given alloy is a strong or a weak ferromagnet as follows (a strong ferromagnet has holes only in the $d\downarrow$ band while a weak ferromagnet has holes and electrons in both $d\uparrow$and $d\downarrow$ bands): $\rho^0_\downarrow$ and $\rho^0_\uparrow$ possesses comparable values for a weak ferromagnet since vacant states are available in both $d\uparrow$and $d\downarrow$ for *s* electrons to make transitions, whereas the values of $\rho^0_\downarrow$ greatly exceeds that of $\rho^0_\uparrow$ in a strong ferromagnet because *s-d* scattering is allowed only for spin down electrons as there are no vacant $d\uparrow$ states at the Fermi level. The variation of SRA with temperature can be understood in the following general terms: As the temperature increased, thermal fluctuations compete with the exchange splitting, leading to equalization in the sub-band occupations, i.e., the difference between the two terms in the numerator of eqn. (3) decreases. This process evolves continuously until T_C is reached, at which point the static exchange splitting collapses and the SRA vanishes. The decrease of the SRA with increasing Mn concentration indicates that the exchange splitting decreases as the Mn concentration increases. From the above discussion, it is tempting to suggest the possible existence of a non-collinear spin structure in

the present series. Particularly, below T_C, the variation of the high-field susceptibility for all samples shows behaviour that is typical for weak-itinerant ferromagnets.

Finally, we focus our attention on the relation between the SRA and magnetization, defined as

$$\left(\frac{\Delta\rho}{\rho_0}\right)_{(s)} = zM^n \quad \text{... (4)}$$

where M is the magnetization taken from the magnetization data and *z* and *n* are constants. Figure 9 shows the relation between the SRA and magnetization for $Fe_{86}Mn_4Zr_{10}$ alloys at different temperatures. The value of *n* increases from 2 in the intermediate-temperature range and has a peak value of approximately (*n*=) 5 around T_C. One may understand this behaviour by considering that as T_C is approached, the effect of the magnetic field on transport properties are dominated by the short range order which would be different from magnetization that is determined by long-range behaviour.

Conclusion

We have studied the temperature and field dependence of magnetization, low-field ac susceptibility and magnetoresistivity of amorphous $Fe_{90-x}Mn_xZr_{10}$ (x=0-16) alloys. These studies indicate that the spin-freezing temperature is affected by Mn substitution. The magnetic parameters obtained from the magnetization data and spontaneous resistive anisotropy data suggest that the antiferromagnetic coupling increases significantly with Mn concentration and results in more frustration which is described in terms of presence of competing exchange interaction between ferromagnetic and antiferromagnetic states. All the samples support the weak-itinerant ferromagnetic nature.

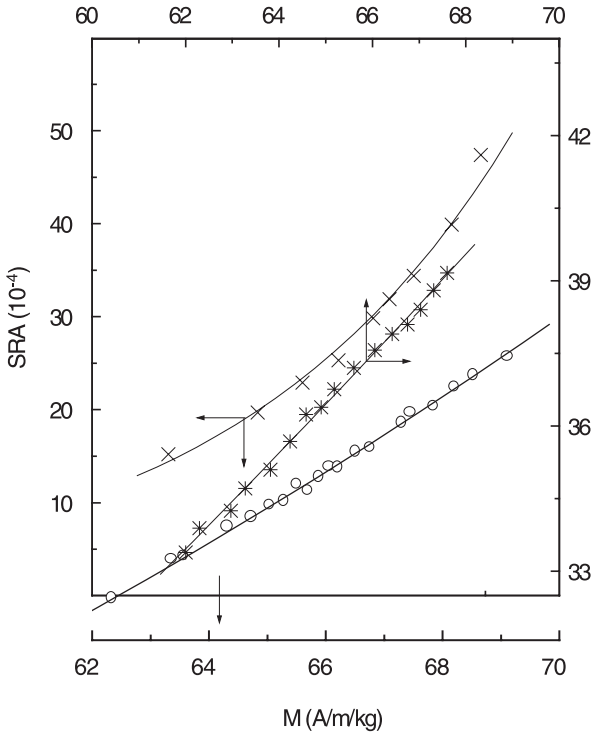

Figure 9: *The relation between spontaneous resistive anisotropy and magnetization at different temperatures 4.2 K (o), 100 K (*) and 200 K (×) for a-$Fe_{86}Mn_4Zr_{10}$ alloy*

Acknowledgement

This work was supported by the Council of Scientific and Industrial Research, New Delhi, INDIA. The author would like to express sincere thanks to Prof. V Srinivas, Physics department, IIT Kharagpur for his valuable discussion and suggestions. The author also acknowledges the support from Korean Basic Science Institute and Chungbuk National University, South Korea for the magnetization measurements.

References

1. K Balakrishnan and SN Kaul *Phys Rev B* **65** (2002) 1334412
2. DH Ryan, JMD Coey, E Battala, Z Altounian and JO Strom-Olsen *Phys Rev B* **35** (1986) 8630
3. SN Kaul, V Sirguri and G Chandra *Phys Rev B* **45** (1992) 12343
4. D Kaptas, T Kemeny, LF Kiss, J Balogh, L Granasy and I Vincze *Phys Rev B* **46** (1992) 6600
5. N Hegman, LF Kiss and T Kemeny *J Phys Condens Matter* **6** (1994) L427
6. Shen Bao-gen, X Rufeng, Z Jiam-gao and Z Wen-shan *Phys Rev B* **43** (1991) 11005 and reference therein
7. A Perumal, V Srinivas, VV Rao and RA Dunlap *Phys Stat Sol (a)* **178** (2000) 783
8. A Perumal, V Srinivas, VV Rao and RA Dunlap *Phys Rev Lett* **91** (2003) 137202
9. L F Barquin, J C Gomez Sal, R Hauser and E Bauer *J Magn Magn Mater* **196-197** (1999) 148
10. K Suzuki, JW Cochrane, A Aoki and JM Cadogan *J Magn Magn Mater* **242-245** (2002) 273
11. A Perumal *Magnetic and Electrical transport properties of Mn substituted Fe-Zr reentrant magnetic glasses* Ph.D. thesis, Indian Institute of Technology Kharagpur, India (2001)
12. A Hernando, V Madurga, MCT Sanchez and M Vanzquez (Eds) *Magnetic properties of amorphous metal* Elsevier, Amsterdam (197) pp 220-244.
13. SN Kaul *Phys Rev B* **27** (1983) 6923
14. H Lerchner and M Rosenberg *Hyperfine Interact*. **39** (1988) 51
15. H Ren and DH Ryan *Phys Rev B* **51** (1995) 15885
16. Y Kakehashi *Phys Rev B* **43** (1991) 10820
17. HS Chen, KT Aust and Y Waseda *J Non-Crys Solid* **46** (1981) 307
18. PL Paulose, S Bhattacharya,V Nagarajan and R Nagarajan *Solid State Commun* **104** (1997) 767
19. D Kaptas, T Kemeny, LF Kiss, J Balogh, L Granasy and I Vincze *Phys Rev B* **46** (1992) 6600
20. AP Malozemoff Phys. Rev. B **32** (1985) 6080